Behavior of Beam to Column Cold-Formed Section Connections Subjected to Bending Moments

Maged T. Hanna

Mohamed M. El-Saadawy

Ghada M. El-Mahdy

Ehab H. A. H. Aly

Wei-Wen Yu International Specialty Conference on Cold-Formed Steel Structures
St. Louis, Missouri, U.S.A., November 7 & 8, 2018

Behavior of Beam to Column Cold Formed Section Connections Subjected to Bending Moments

Maged T. Hanna[1], Mohamed M. El-Saadawy [1],
Ghada M. El-Mahdy[1], Ehab H. A. H. Aly [1]

Abstract

Cold formed sections are often used in the construction of mid-rise buildings due to their high strength weight ratios, and fast erection. In these buildings, the connections between joists and studs are mainly simple connections. However, application of these sections can be extended to moderate span frames where connections between members are subjected to bending moments. Strength and stability of such frames depends to large extent on the behaviour of the connections between their members. Over the last twenty years, several researchers undertake tests on cold formed section connections subjected to bending moments. Major of them classify the connections as semi-rigid, but some suggested that as we reach the maximum capacity of the connected sections so we can consider it rigid.

[1] Professor of Steel Structures, Housing and Building National Research center, Egypt

In this paper, experimental investigations are carried out to study the structural response of two cold formed section connections subjected to bending moments. In the first type, the beam is connected to the column via bracket plate attached to the web of the beam and column sections, whereas, in the second type, flanges of the connected beams and columns are joined together by additional plate at the tension and compression side. Lipped channel sections with dimensions of 200 mm for the web, 60 mm for the flanges, and 20 mm for the lip are studied. Moreover, the experimental set-up is simulated numerically using a non-linear finite element model. The cold-formed sections are modeled using shell elements while the connecting fasteners are modeled using beam elements.

Introduction

Steel cold-formed sections (CFS) have traditionally been used as purlins and side girts for industrial buildings. However, recently the use of steel CFS has been extended to primary members in the construction of low to medium rise houses and portal frames with moderate spans. The use of steel CFS for columns and rafters of short and moderate span portal frames could be an economic alternative to conventional hot rolled or built up sections. The design of such frames will depend largely on the nature (rigid/semi-rigid) of the connection between the rafter and the column. Previous research [Chung and Lau (1999), Lim and Nethercot (2004), Elkersh (2010), and Öztürk and Pul (2015)] has shown that the main problem with using CFS in portal frames is the semi-rigidity of the connections due to bolt hole elongation. This reduces the moment carrying capacity of the connection [Wong and Chung (2002), Lim and Nethercot (2003), Dundu and Kemp (2006), and Jackson *et al.* (2012)]. The behaviour of eave and ridge joints of CFS portal frames was also studied by Dubina *et al.* (2004) and the study was extended to the experimental testing of full scale portal frames [Dubina *et al.* (2009)].

The motivation behind this study is to investigate the carrying capacities of single lipped channel cold formed section screw fastened connections subjected to major axis bending moments. For this purpose, cantilever beam is connected to a vertical column as depicted in Fig. 1. The beam is subjected to vertical concentrated load at its free end. The cross section dimensions of the beam and column sections are similar, and equal to 200mm, 60mm, 20mm for the web height, flange width, and lip depth; respectively. The main parameters of the study are the thickness of the channel section, t_1, and the thickness of the gusset plates, t_2.

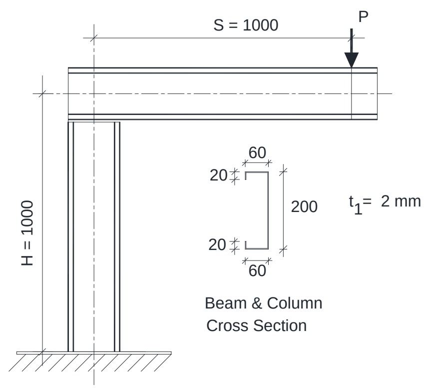

Fig. 1: Case of Study

Experimental Work

Specimen Dimensions and Material properties

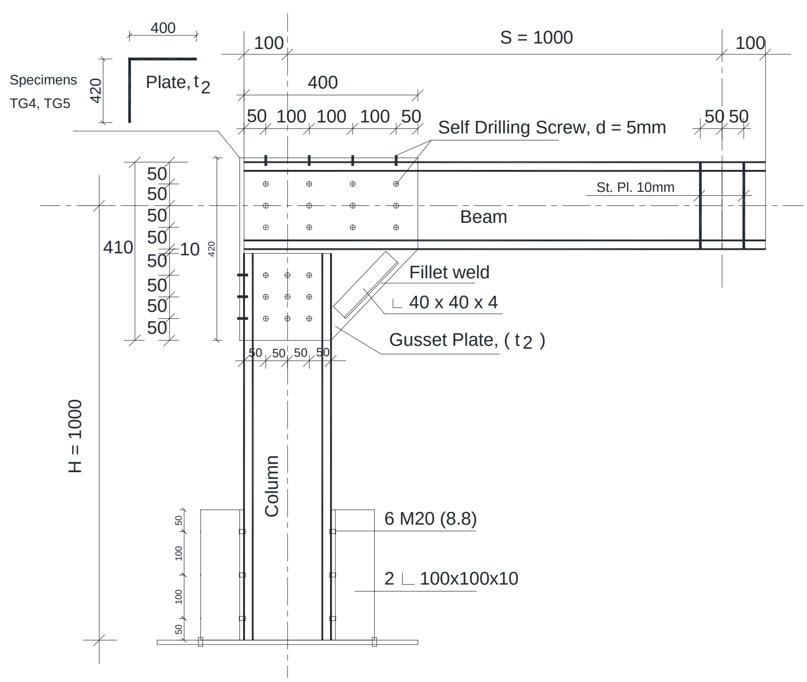

Fig. 2: Specimens connected with tapered gusset plate, TG1, TG1m, TG2, TG3,TG4,TG5.

This study involves tests of ten specimens. Geometry of the tested specimens are shown in Figs. 2 & 3, and listed in table 1. In the first specimen, TG1, the beams are joined to the column by a tapered gusset plate connected to the web of each member. In the next specimens, TG1m, TG2 & TG3, an equal angle with dimensions 40x40x4 mm is welded to the inclined part of the tapered connecting plate to prevent local buckling in this part. In specimens, TG4 & TG5 an additional bent plate is used to connect the tension flanges of the beam and the column together. However, beams and columns in specimens RG1 & RG2 are connected by rectangle gusset plate with width equal to the height of the column web. Also, additional bent plates are used to connect tension and compression flanges in specimens RG3 & RG4. Hex washer head screw with diameter of 5mm is used in the connection. There is thick base plate connected to the specimen columns by vertical angles that are welded to the base plate.

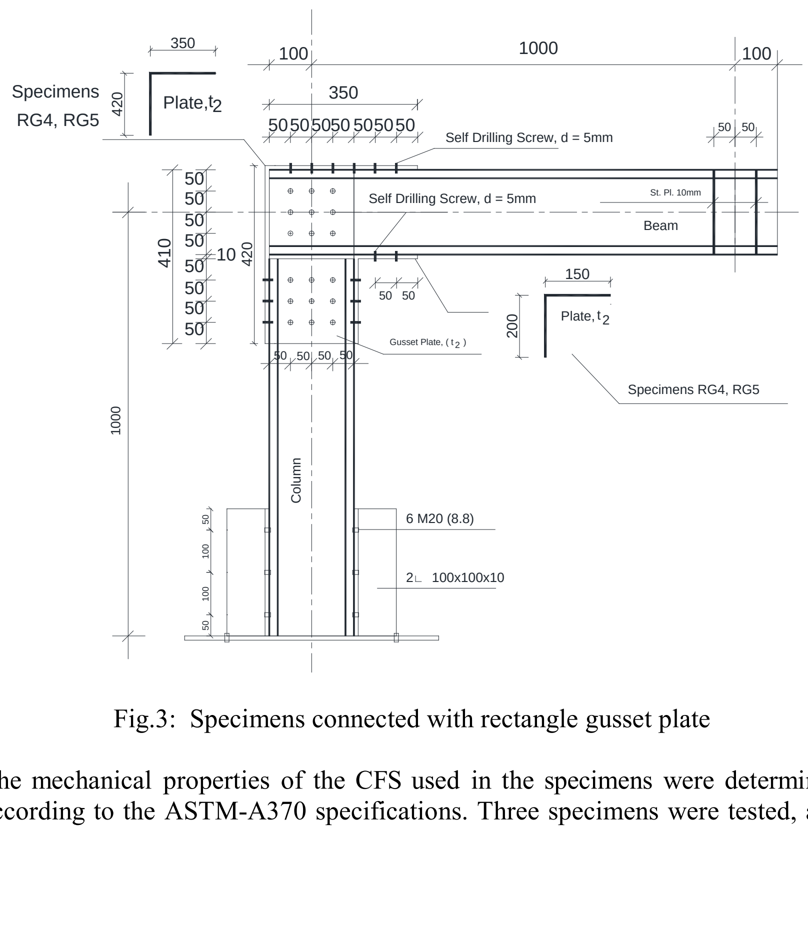

Fig.3: Specimens connected with rectangle gusset plate

The mechanical properties of the CFS used in the specimens were determined according to the ASTM-A370 specifications. Three specimens were tested, and results revel that the steel is high strength steel with yield stresses and Young's modulus equal to 450MPa, and 210000 MPa; respectively. Moreover, To determine the shear strength of the screw, three single shear specimens were tested as shown in Fig.4. The connection was done using a single hex-washer head, 5 mm diameter screw. In this specimen, the connecting plate thickness were 4mm. All the three specimens were failed by shear in the screw at stresses equal to 720 MPa. Figure 4 illustrate the screw single shear test and the failure shape

Specimen in the Test Machine Specimen after test pure Shear failure

Fig.4: Single shear test of the hex washer head screw

Table 1: Test specimens measured dimensions and results

Spec.	Measured Dimensions		gusset plate thickness, t_2, (mm)	Experimental		Finite Element Analysis	
	H (mm)	S (mm)		P_u (KN)	M_u/M_s	P_u (KN)	M_u/M_s
TG1	998	993	2.8	8.9	0.382	8.4	0.37
TG1m	995	993	2.8	15.4	0.688	14.1	0.62
TG2	992	995	2.95	17.1	0.76	16.1	0.72
TG3	1003	992	2.95	16.7	0.74	16.2	0.72
TG4	998	996	3.8	16.9	0.75	17.1	0.76
TG5	995	1003	3.8	17.4	0.77	17.1	0.76
RG1	993	998	2.9	9.3	0.48	8.3	0.43
RG2	1003	1001	2.9	11.3	0.59	11.1	0.59
RG3	995	996	3.95	12.1	0.63	12.8	0.67
RG4	1002	998	3.95	14.5	0.76	14.8	0.77

Note: measured thickness of the cold formed section, t_1 = 2.3mm

Test Setup

The specimens were fixed in a reaction frame through thick base plate by four bolts with diameter 20mm and grade 8.8. Slot holes were done in the plate to adjust the specimens so that the vertical loads applied through the shear center of the cross section. Monotonic load applied vertically by 50 ton hydraulic jack. Two vertical stiffeners with thickness of 10mm each welded to the specimen in the section where the load was applied to prevent crippling in this zone. To prevent the out of plane deformation of the specimens, lateral restraints attached to the specimens at the tip of the horizontal beam below the load application, and at the mid span of the cantilever beam. This was done by passing the specimen through wooden boxes that are laterally connected to steel road which move inside vertical slot. The used box has length of 150mm, and inside dimensions similar to the beam cross section. Hence, this configuration allows the vertical in plane displacement of the specimen beam, and prevent the out of plane deformations. Test setup is illustrated in Fig. 5.

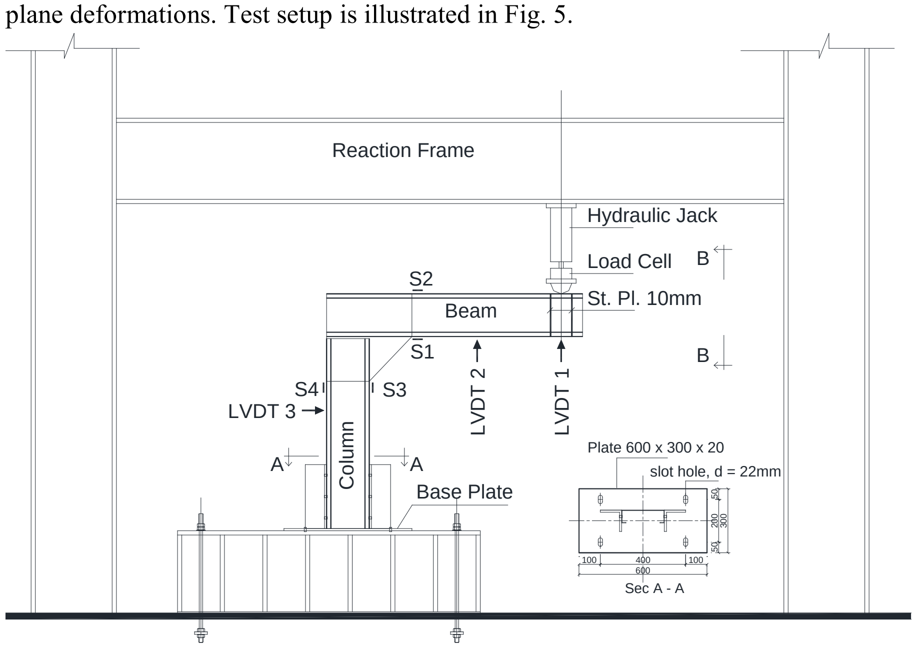

Fig.5: Schematic Diagram For the Test Setup

The in plane deformations of the specimens were measured through linear variable displacement transducers (LVDT) with accuracy of 0.01 mm. The

measured points were the vertical displacements of the beam end section below the load application (LVDT 1), as well as the beam mid-length section (LVDT 2). In addition, the horizontal displacement of the mid-height section of the column was recorded (LVDT 3).
The LVDT readings were collected using a data acquisition system. In addition four strain gages were attached to the specimens to measure the tension as well as the compression flange strains at sections just before the connection in the specimen beam column. An arbitrary increment of load equal to 5kN was applied, and then the load was held constant until stable readings were recorded. This procedure was repeated for each additional load increment until excessive deflections were observed without any increase in the applied load. Thus, the ultimate load was achieved.

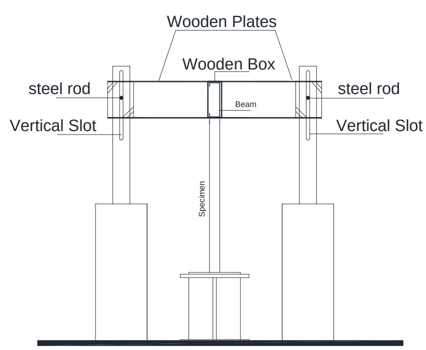

View B-B in Fig. 5

Photo showing the test setup

Fig.6: Schematic Diagram For the Test Setup

Numerical Simulation

A non-linear finite element model is made using the general purpose finite element software package ANSYS Launcher 11. Four nodes isoparametric shell element, SHELL181, is used in this model. It is a 4-node element with six degrees of freedom at each node. Further, this element allows for for both geometric and material nonlinearties. The mesh density is chosen to make the element aspect ratio on average equal to 1. In addition, the BEAM4 element was used to model the screws that connect beam and column cross sections to the gusset plate.

The material properties were taken from the tensile coupon test results. The nominal yield stress, F_y, of steel was taken as 4.5 t/cm^2 (450 MPa) and the ultimate strength, F_u, was taken as 5.4 t/cm^2 (540 MPa). Young's modulus of elasticity, E, and shear modulus, G, are 2100 t/cm^2 (210 GPa), 810 t/cm^2 (81 GPa); respectively. ANSYS classical metal plasticity model was used to include the material non-linearity effects. This model implements the von-Mises yield surface to define isotropic yielding and associated plastic flow theory. A perfect plasticity model based on a simplified bilinear stress-strain curve without strain hardening was assumed. Figure 7 shows the finite element model, loads, and boundary conditions.

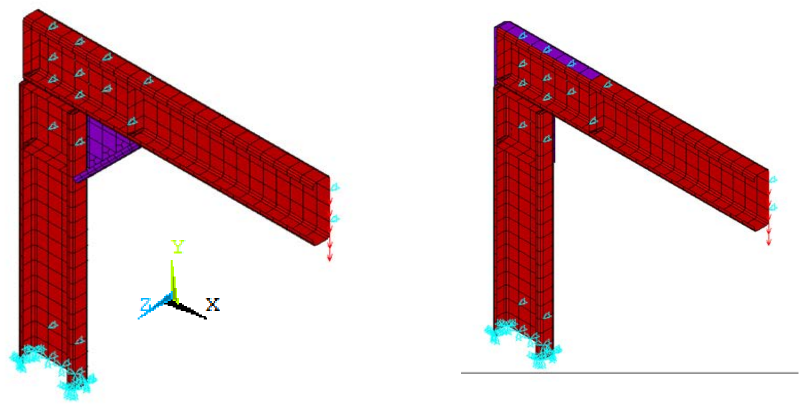

Specimens with tapered gusset   Specimens with rectangle gusset

Fig.7: Finite Element Model

The base conditions for the column elastic line were treated as fixed condition. Therefore, all joints at the column base were prevented from translation along X, Y, and Z axis. Due to the presence of lateral restraints at the beam mid length section as well as beam free end section, joints of the flange web and flange lip juncture of these sections are prevented from translation along Z-axis (out of plane direction). In addition joints of the web at the beam end section where loads are applied are prevented from translation along Z axis to represent the presence of the vertical stiffener at this section. To prevent the crippling of the web, Loads are distributed along the web joints at the beam free end. Loads were incrementally increased through successive load steps. Newton-Raphson iterations were used in solving the nonlinear system of equations.

Results

To assess the behavior of the studied connections, the applied moment, M_u, has been normalized with respect to the flexural capacity of the beam section, M_s. Hence, the ratios M_u/M_s are plotted versus the generalized displacements and strains. The applied moments are calculated as the result of the multplication of the applied load, P, and distance between the load and the center of the screws that connect the gusset with the web of the beam section. The section flexural capacity, M_s, is calculated using DSM, in which the flexural strength will be the minimum of the local, distortional, and the overall buckling strength. This method requires the calculation of the elastic critical local and distortional buckling stresses, these values have been determined using CUFSM computer program.

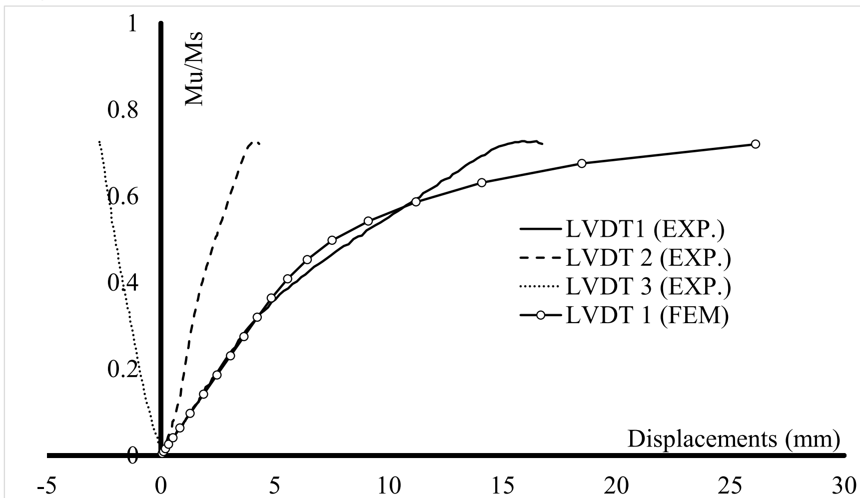

Fig. 8: M_u/M_s versus displacements for specimen TG2

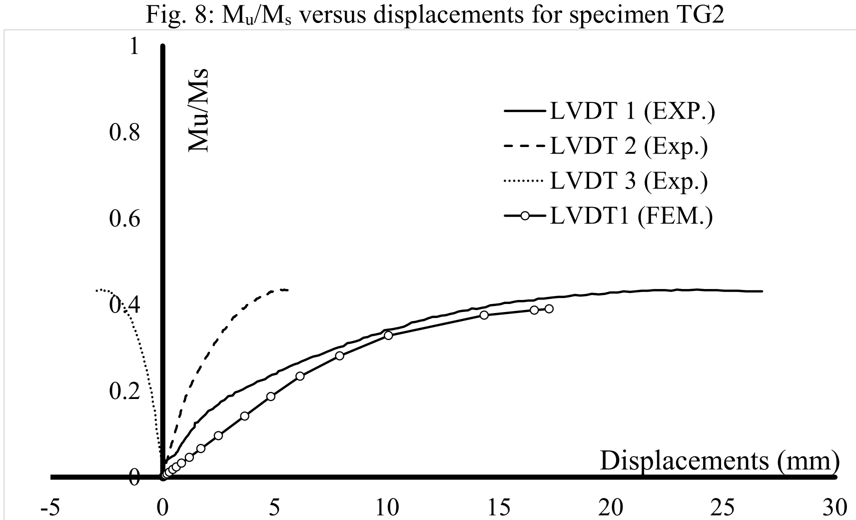

Fig.9: M_u/M_s versus displacements for specimen RG1

The ratios M_u/M_s are drawn with respect to the displacements of the three measured points of specimens TG2 and RG1 in Fig 8 and Fig. 9; respectively. It is obvious that the relations are almost linear at the early stages of loading, then near failure the structural response become nonlinear and the stiffness decreases continuously. In addition, the numerical finite element results are plotted in the same figure for point 1. It is clear that there is good correlation between numerical and experimental results.

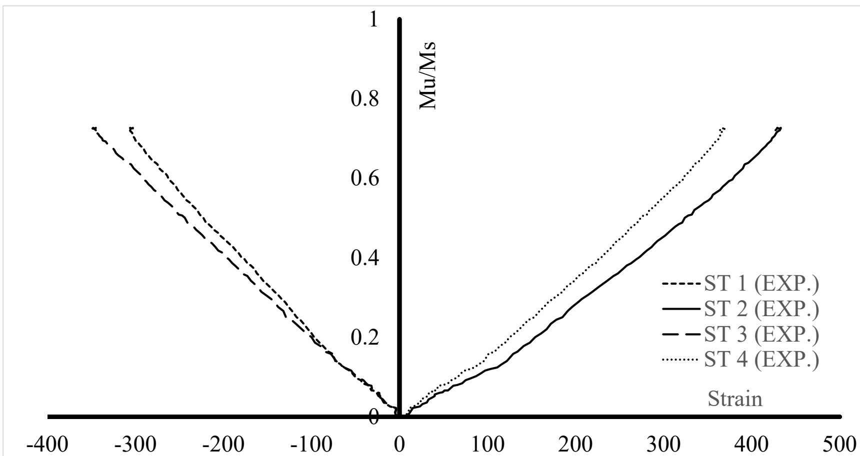

Fig 10: M_u/M_s versus longitudinal strains for specimen TG2

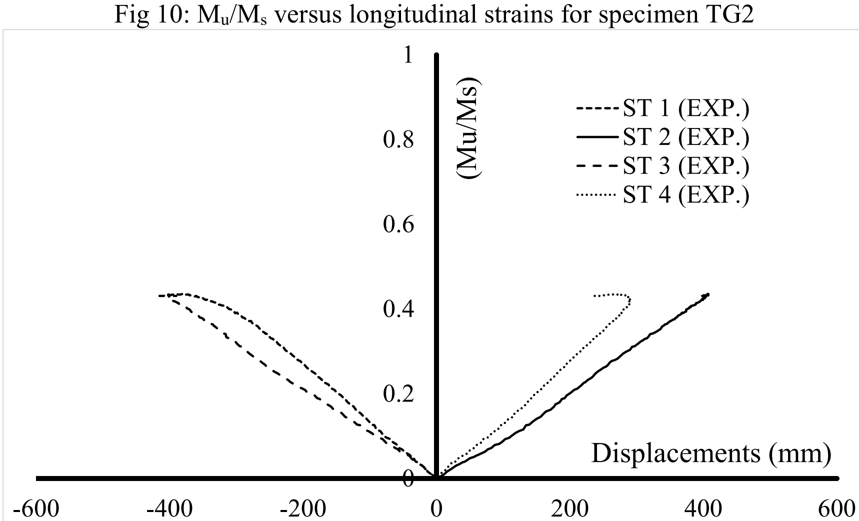

Fig 11: M_u/M_s versus longitudinal strains for specimen RG1

The load strain relationships are also examined. Therefore, the ratios M_u/M_s are plotted with respect to the longitudinal strains of the tension as well as compression flanges of the beam and column sections in Fig. 10 for specimen TG2. However, results of specimen RG1are shown in Fig. 11. It is clear that the strains are linear until failure. To add on the tensile and compressive strains in the beam section are almost similar. However, in column sections the tensile strains are smaller than the compressive strain due to the presence of the axial compressive force. This means that the longitudinal strains are transformed from the beam section to the columns section through the tapered as well as the rectangular gusset plates.

The ratios M_u/M_s are drawn with respect to the vertical displacements of point 1 for all specimens with tapered gusset plate in Fig. 12, and for specimens with rectangle gusset plate in Fig. 13. The results are also listed in Table 1. It is obvious that specimens with tapered gusset plate reaches about 80 % of the section flexural capacity, except specimen TG1 where failure happened when M_u/M_s reaches about 38%. This is because, this specimen fail when the gusset buckle at small level of loads. On the other hand, specimens with rectangle gusset plate reache about 60 % of the flexural capacity of the beam sections. For the two types of connections changing thickness of the gusset plate does not significantly change the ultimate capacity, but it reduces the displacements at the ultimate loads. Also, using plates connecting tension and compression flanges improve the performance of the connections with rectangular web.

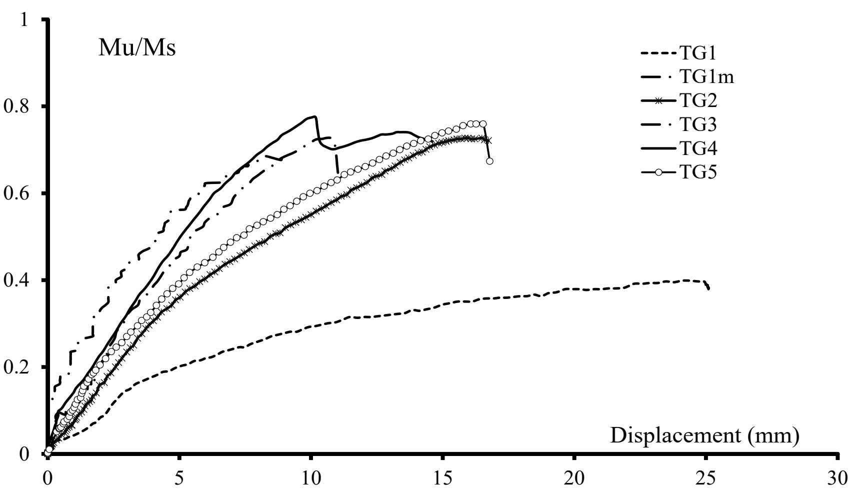

Fig. 12: Mu/Ms versus vertical displacements of point 1
(specimens TG1, TG1M, TG2, TG3, TG4,TG5)

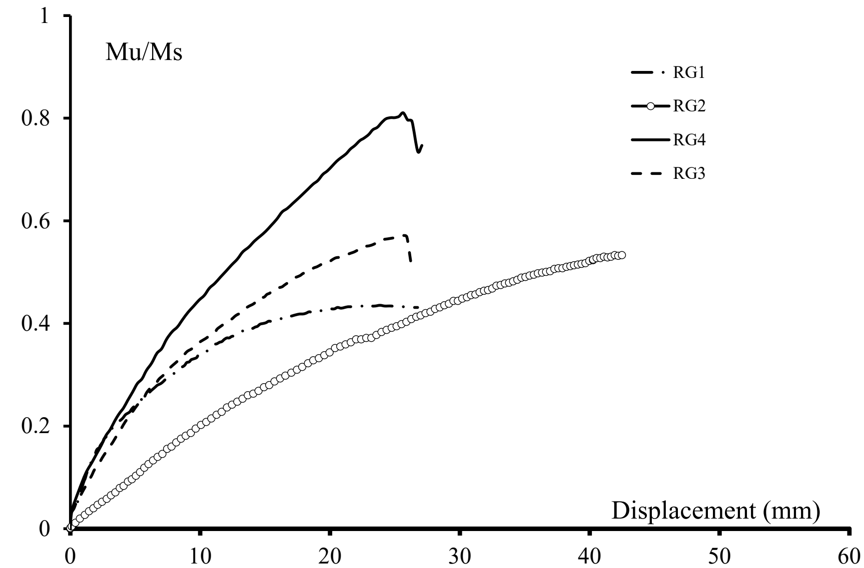

Fig. 13: M_u/M_s versus vertical displacements of point 1
(specimens RG1, RG2, RG3, RG4)

Small rotation in the beam

Tilting in the screw and bearing in the plate

Fig. 14: Failure Shape of Specimen TG2

In plane bending associated with small amount of rotation about the beam longitudinal axis is noticed at failure. The beam exhibit some rotation at failure because the applied loads were not exactly at the section shear center in addition to the gap between the beam cross section and the wooden boxes used to make the lateral restraints. Moreover, tilting in the screw and bearing in the beam web was observed. Failure shape of specimens TG2 are depicted in Fig. 14. Also Fig. 15 shows the failure mode obtained in the numerical finite element model.

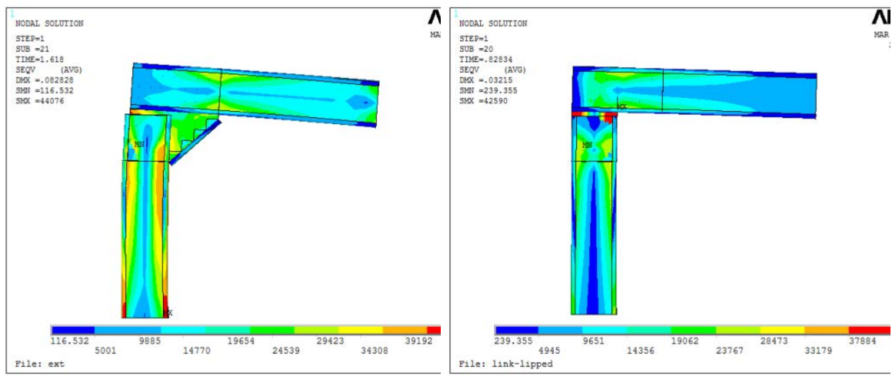

Specimen TG2 Specimen RG1

Fig.15: Numerical failure shape

Conclusions

In this study experimental and numerical investigation are carried out for the behavior of beam to column single lipped channel cold formed section screw fastened connections subjected to major axis bending moments. Group of connections were done using tapered gusset plates, while in the other group the tapered gusset plate are replaced by rectangle one. Results revel that the numerical and experimental ultimate loads as well as failure modes are comparable. Moreover, specimens with tapered gusset plate reaches about 80 % of the beam section flexural capacity. However, for specimens with rectangle gusset plate this ratio become 60 %. Further, the longitudinal strains are transformed from the beam section to the columns section through the tapered as well as the rectangular gusset plates. For the two types of connections changing thickness of the gusset plate does not significantly change the ultimate capacity, but it reduces the displacements at the ultimate loads. Also, using plates connecting tension and compression flanges improve the performance of the connections with rectangular web.

Acknowledgments
Authors acknowledge Ahmed Massoud, under graduate student at British University in Egypt (BUE), civil engineering department for his effort in the lab during tests, collecting data, and presenting results.

References

ANSYS Launcher 11 (2007), ANSYS Inc., Canonsburg, PA, USA, ansys.com.

Chung, K.F. and Lau, L. (1999). Experimental investigation on bolted moment connections among cold formed steel members. Engineering Structures, 21(10):898-911.

CUFSM V3.12, "Elastic Buckling Analysis of Thin-Walled Members by Finite Strip Analysis", http://www.ce.jhu.edu/bschafer/cufsm

Dubina, D., Stratan, A., Ciutina, A., Fulop, L., and Nagy, Z. (2004). Performance of ridge and eaves joints in cold-formed steel portal frames. Proceedings of the 17th International Conference on Cold-Formed Steel Structures, Orlando, Florida, U.S.A.

Dubina, D., Stratan, A., Nagy, Z. (2009). Full-scale tests on cold-formed steel pitched-roof portal frames with bolted joints. Advanced Steel Construction, 5(2):175-194.

Dundu, M. and Kemp, A.R. (2006). Strength requirements of single cold-formed channel sections connected back-to-back. Journal of Constructional Steel Research, 62:250-261.

ECP (2001). Egyptian Code of Practice for Steel Construction and Bridges – Allowable Stress Design.

Elkersh, I. (2010). Experimental investigation of bolted cold formed steel frame apex connections under pure moment. Ain Shams Engineering Journal, 1:11-20.

Hanna, M.T. (2014). Structural performance of steel cold formed sections portal frames. Proceedings of the 7th European Conference on Steel and Composite Structures, Napoli, Italy.

Jackson, C., Wrzesien, A.M., Johnston, R.P., Uzzaman, A., and Lim, J.B.P. (2012). Effect of reduced joint strength and semi-rigid joints on cold-formed steel portal frames. Proceedings of the 6th International Conference of Coupled Instabilities in Metal Structures, Glasgow, U.K.

Lim, J.B.P. and Nethercot, D.A. (2003). Ultimate strength of bolted moment connections between cold-formed steel members. Thin-Walled Structures, 41:1019-1039.

Lim, J.B.P. and Nethercot, D.A. (2004). Stiffness prediction for bolted moment connections between cold-formed steel members. Journal of Constructional Steel Research, 60:85-107.

Öztürk, F. and Pul, S. (2015). Experimental and numerical study on a full scale apex connection of cold-formed steel portal frames. Thin-Walled Structures, 94:79-88.

Pernes, P.M. and Nagy, Z. (2012). FE modeling of cold-formed steel bolted joints in pitch-roof portal frames. ActaTechnicaNapocensis: Civil Engineering & Architecture Vol. 55, No. 3.

Wong, M.F. and Chung, K.F. (2002). Structural behaviour of bolted moment connections in cold-formed steel beam-column sub-frames. Journal of Constructional Steel Research, 58(2):253-274.

Schafer BW, "Design Manual for the Direct Strength Method of Cold-formed Steel Design", Final Report to the American Iron and Steel Institute, Washington, DC, 2002